JOURNAL OF GEOPHYSICAL RESEARCH, VOL. 103, NO. C13, PAGES 30,973–30,984, DECEMBER 15, 1998

Flow of Bottom and Deep Water in the Amirante Passage and Mascarene Basin

Gregory C. Johnson,[1] David L. Musgrave,[2] Bruce A. Warren,[3] Amy Ffield,[4] and Donald B. Olson[5]

Abstract. In the Indian Ocean the Amirante Passage is the sill through which relatively cold, fresh, oxygen-rich, and nutrient-poor bottom water spreads northward into the Somali Basin from the Mascarene Basin. The passage is also a conduit through which relatively warm, salty, oxygen-poor, and nutrient-rich deep water spreads south. Previous estimates for northward transport of bottom water in the passage have been made from station pairs and sections without benefit of tracer measurements. Previous estimates of southward transport of deep water are scarce. Three hydrographic sections were made across the passage in 1995 and 1996 as part of the World Ocean Circulation Experiment (WOCE). Two WOCE sections were also made perpendicular to the western boundary in the Mascarene Basin, just south of the passage. The geostrophic shear field is used with the salinity, dissolved oxygen, and silica distributions to select a range of zero-velocity surfaces (ZVSs) on potential isotherms from 1.0° to 1.1°C (hence a range of geostrophic transports) for which the flow direction is consistent with the tracer distributions. Objective mapping is used to obtain flux estimates below the deepest common level of station pairs. Estimates in the Mascarene Basin result in a bottom water volume transport from 2.5 to 3.8 $\times$ 10^6 m^3 s^{-1} northward toward the passage below the ZVSs and a deep-water transport between the ZVSs and 2.5°C from 11.6 to 6.4 $\times$ 10^6 m^3 s^{-1} southward. Estimates within the passage result in transports from 1.0 to 1.7 $\times$ 10^6 m^3 s^{-1} northward for the bottom water and from 8.6 to 3.8 $\times$ 10^6 m^3 s^{-1} southward for the deep water.

1. Introduction

A powerful dynamical framework for the large-scale abyssal circulation consists of interior upwelling fed by high-latitude sinking through deep western-boundary currents [*Stommel and Arons*, 1960]. In the South Indian Ocean, zonal hydrographic sections have revealed three separate northward flows in deep western-boundary currents supported by three roughly meridional boundaries defined by continental rises and ocean ridges that separate the Indian Ocean into three sets of deep basins [*Warren*, 1981; *Toole and Warren*, 1993]. Maps of water properties on, and depths of, potential-density surfaces illustrate some aspects of these flow patterns, especially the large-scale control by bottom topography [*Mantyla and Reid*, 1995].

Estimates of net transport below about 2000 dbar into the Indian Ocean near 32°S range from a minimum of zero as derived from hydrographic stations so sparse as to miss the boundary currents [*Fu*, 1986], as well as from a combination of heavily smoothed climatology with a general-circulation model [*Lee and Marotzke*, 1997], to a maximum of 27 $\times$ 10^6 m^3 s^{-1} as derived from a closely spaced hydrographic section with the zero-velocity surface (ZVS) for geostrophic-velocity computation inferred from water-property distributions [*Toole and Warren*, 1993]. The most recent observation-based estimate for the total northward flow of abyssal waters into the Indian Ocean across 32°S latitude [*Robbins and Toole*, 1997] is 11.9 $\pm$ 2.7 $\times$ 10^9 kg s^{-1} (converting mass transport to volume transport involves dividing by the in situ density, so 10^9 kg s^{-1} $\approx$ 10^6 m^3 s^{-1}), obtained by using the silica budget to adjust the reference velocities of *Toole and Warren* [1993]. Further quantifying the northward mass and property fluxes of the abyssal flow, and the return fluxes southward, will help to elucidate the role that the thermohaline circulation in the

[1]Pacific Marine Environmental Laboratory, NOAA, Seattle, Washington.

[2]University of Alaska Fairbanks/SFOS.

[3]Department of Physical Oceanography, Woods Hole Oceanographic Institution, Woods Hole, Massachusetts.

[4]Lamont-Doherty Earth Observatory, Columbia University, Palisades, New York.

[5]Rosenstiel School of Marine and Atmospheric Science, University of Miami, Miami, Florida.

Copyright 1998 by the American Geophysical Union.

Paper number 1998JC900027.
0148-0227/98/1998JC900027$09.00

Indian Ocean plays in global heat and freshwater budgets.

The western series of deep basins in the Indian Ocean, from south to north, consists of the Crozet, Madagascar, Mascarene, Somali, and Arabian Basins (Figure 1). There are at least twelve published studies using sixteen hydrographic sections spanning part or all of these western basins to make geostrophic transport estimates for northward abyssal flow (Table 1). These estimates start at 7–11 $\times$ 10^6 m^3 s^{-1} at 32°S and generally decrease northward to 1–5 $\times$ 10^6 m^3 s^{-1} near and north of the Amirante Passage (9°S, 53°E), the deepest connection between the Mascarene and Somali Basins, near 9°S, 53°E (Figure 1). ZVSs for these estimates range between 1000 and 4200 dbar, tending to deepen from south to north and from west to east. For many of these transport estimates, visual inspection of potential temperature or density sections suggests that the ZVS choices are made to maximize northward baroclinic velocity in the bottom water, assuming a middepth zero-velocity surface.

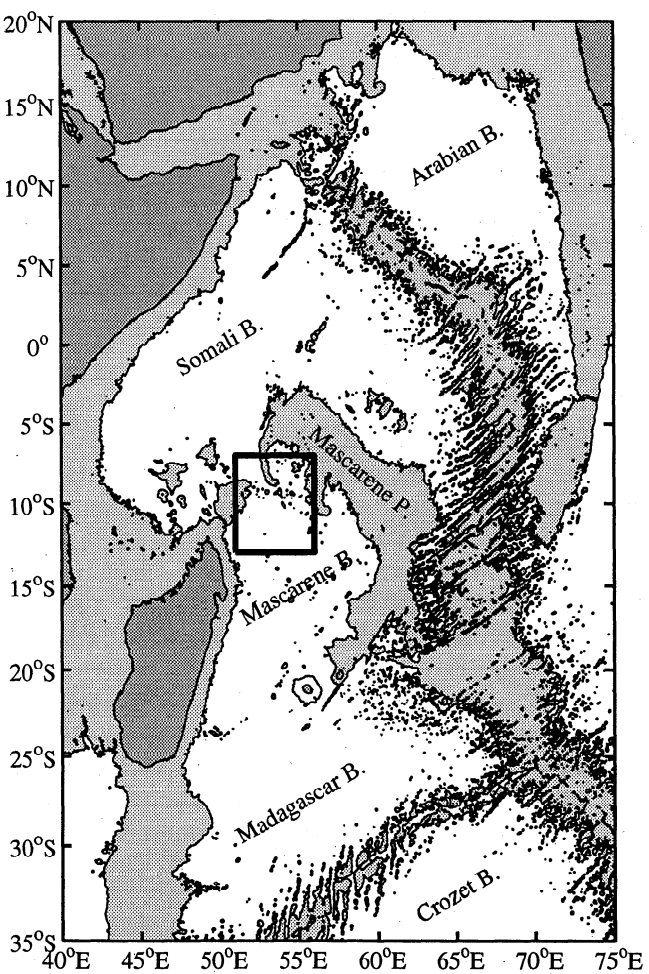

Figure 1. Map (Mercator projection) of the western Indian Ocean with basin names and the 3650-m isobath (thin line) [*Smith and Sandwell*, 1997] that defines the Somali Basin. The location around the Amirante Passage (inside thick line) is shown in detail in Figure 2.

Two of the twelve studies and five of the sixteen hydrographic transport estimates of abyssal flow in the western basins (Table 1) are across the Amirante Passage. The 3650-m isobath [*Smith and Sandwell*, 1997] encloses the Somali Basin (Figure 1) except for the Amirante Passage to the south and the Owen Fracture Zone (10°N, 57°E) to the north. Thus the Amirante Passage is the route by which all bottom water from the south enters the Somali Basin. All previous bottom water transports in the passage are calculated relative to and below a 3800-dbar ZVS, a choice which, for a deep ZVS above the passage, generally maximizes northward transport of bottom water. Two of these estimates are actually made using two sets of station pairs within the passage which each yield ranges of relatively small transport estimates [*Fieux and Swallow*, 1988]. For these estimates, geostrophic velocity is extrapolated as a constant below the deepest common level (4200 dbar) for the station pairs, but different assumptions about where this flow is located above the highly varying topography leads to different values for the resulting transport increments, and hence for the ranges in the total estimates. The extrapolations account for 0.3–1.1 $\times$ 10^6 m^3 s^{-1} and 0.1–1.3 $\times$ 10^6 m^3 s^{-1} of these transport estimates. The other three transports are based on sections of four to six stations each within the passage [*Barton and Hill*, 1989]. These higher-resolution sections more than double the transport estimates obtained from the station pairs. Extrapolation of velocities below the deepest common levels in these sections accounts for 0.9, 3.6, and 1.5 $\times$ 10^6 m^3 s^{-1} of the transport estimates. Thus, while the distribution of geostrophic velocities across the passage is better defined by the sections than by the station pairs, in both cases the extrapolated velocity accounts for roughly half the transport estimate.

This investigation examines three recent, densely sampled hydrographic sections that span the entire Amirante Passage, together with the three sections previously analyzed by *Barton and Hill* [1989], and includes two more just south of the passage in the Mascarene Basin. This regional analysis of deep and bottom water transports improves on previous studies in four ways. First, estimates of transport below the deepest common level of station pairs are achieved through objective mapping rather than assuming a uniform velocity, making consistent use of all the hydrographic information gathered. Second, water property distributions are combined with the geostrophic shear to select a plausible range of ZVSs, again incorporating more information than was used in previous studies. Third, the boundary between bottom and deep water is defined as the ZVS, and the upper limit of deep water is set by examination of the water property distributions. This procedure achieves improved estimates of northward transport of bottom water, as well as estimates of southward transport of deep water in the region. Fourth, the relatively large number of sections an-

Table 1. Summary of Published Northward Deep Transport Estimates in the Western Basins of the Indian Ocean, Proceeding From South to North

Location	Lat., °S	ZVS, dbar	Transport, 10^6 m^3 s^{-1}	Comments	Reference
Crozet Basin	48	2500	3.2	>ZVS	*Warren* [1978]
Madagascar and Crozet Basins	32	1000–3600	11.0	>2000 dbar	*Toole and Warren* [1993]
Madagascar and Crozet Basins	32	1000–3600	7.4*	>~2000 dbar, silica constraint	*Robbins and Toole* [1997]
Southwest Indian Ridge	32–23	3500 m	6.1	>ZVS, along ridge	*Warren* [1978]
Madagascar Basin	35–20	3500 m	5.2	>ZVS, nonzonal	*Swallow and Pollard* [1988]
Madagascar Basin	23	3100	5.7	>ZVS	*Warren* [1974]
Madagascar Basin	23	3100	3.6	>ZVS, repeat section	*Fieux et al.* [1986]
Mascarene Basin	18	1400–4200	5.2	>2000 dbar, DWBC only	*Warren* [1981]
Mascarene Basin	12	3600	4.4	>ZVS	*Warren* [1974]
Amirante Passage	9	3800	0.8–2.1 and 0.9–1.7	>ZVS, two sets of station pairs	*Fieux and Swallow* [1988]
Amirante Passage	9	3800	3.7, 5.1, and 2.8	>ZVS, three sections	*Barton and Hill* [1989]
Somali Basin	4–2	1.2°C θ	3.2 and 4.6	>ZVS, two sections, DWBC only	*Johnson et al.* [1991b]
Arabian Basin	12°N	3000	3.2, 2.3, and 1.2	>ZVS, three sections	*Quadfasel et al.* [1997]
Arabian Basin	7°–10°N	1.7°C θ	0.5 and 4.8	>ZVS, two sections, DWBC only	*Johnson et al.* [1991a]

ZVS, zero-velocity surface; DWBC, deep western-boundary current. The third study is a reanalysis of the second, otherwise, different hydrographic data sets are used for each estimate. Most of these studies assume a constant velocity below the deepest common level of each station pair.

*10^9 kg s^{-1}.

alyzed, with closely spaced stations, allows for improved statistical uncertainties in the transport estimates.

2. Data and Mapping

As part of the U.S. component of the World Ocean Circulation Experiment (WOCE), three hydrographic sections were occupied across the entire Amirante Passage and two sections just south of the passage in the Mascarene Basin (Figure 2). Data examined are continuous conductivity-temperature-depth (CTD) profiles of temperature T and salinity S versus pressure P, together with discrete bottle measurements of dissolved oxygen, O_2, and silica, H_4SiO_4, at selected pressures. Stations used here for volume transport calculations include 70–91 from cruise IR7N, occupied in April 1995, stations 720–738 from cruise I7N, occupied in July 1995, and stations 1197–1215 from I2, occupied in January 1996. The mean station spacing is 37 km, the minimum is 11 km, and the maximum is 75 km. Stations were occupied to within 10 m of the bottom. These CTD profiles and discrete bottle data are preliminary but are already thought to comply with WOCE one-time survey standards for accuracy and precision (T. Joyce and C. Corry, Requirements for WOCE hydrographic programme data reporting, unpublished manuscript, 1994) and are not likely to change much when final calibrations are completed. In addition, the CTD data from three sections (Figure 2; CD22, CD24, and CD24S) taken across the passage in April and June of 1987 [*Barton and Hill*, 1989] are reanalyzed here. Potential temperature θ, in situ density, and specific volume anomaly are calculated from the 2-dbar CTD data, filtered with a 50-dbar half-width Hanning filter, and subsampled at 50-dbar intervals. The square of buoyancy frequency, $N^2 = g/\rho\ \partial\rho/\partial z$, is also calculated from the 2-dbar CTD data. Here g is the local gravitational acceleration and the density ρ is locally referenced to the central pressure over which the derivative is evaluated; hence the effect of compressibility is excluded but that of the adiabatic temperature gradient is included. The N^2 estimates are filtered with a 250-dbar half-width Hanning filter before subsampling because, as derivatives, they are inherently noisy.

Geostrophic flux calculations use horizontal specific volume anomaly gradients between station pairs. In regions where the bottom slopes, this means that some ad hoc method (usually applying zero velocity, a constant velocity from above, or a constant vertical shear from above) is often used to extend these calculations below the deepest common level of station pairs, into what are customarily called the bottom triangles. Instead of this ad hoc procedure, here water properties in these regions are extrapolated systematically using objective mapping techniques [*Roemmich*, 1983]. The power of the method is in the combined use of vertical and hor-

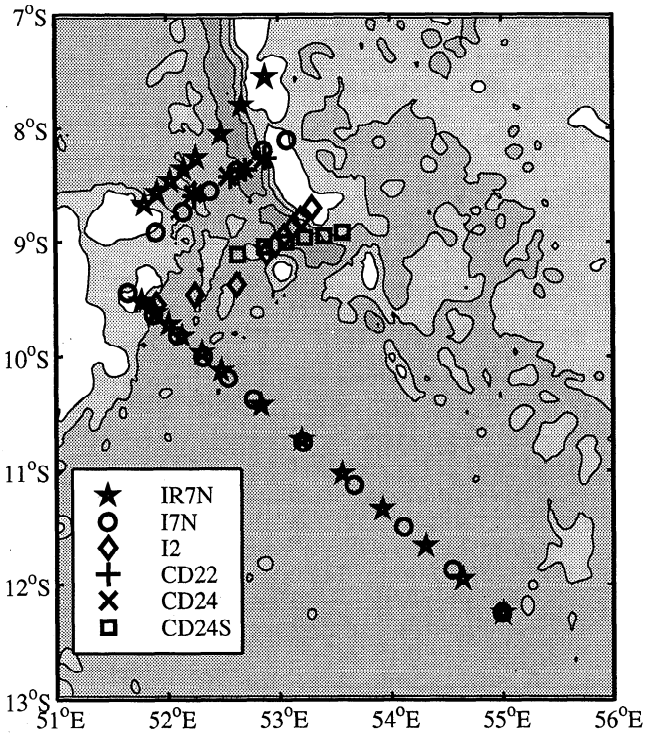

Figure 2. Detailed map (Mercator projection) in the Amirante Passage (near 9°S, 53°E) region with areas between 3000-m, 4000-m, and 5000-m isobaths (black) increasingly shaded [*Smith and Sandwell*, 1997] and station locations (see legend). See Figure 1 for map location within western Indian Ocean. Sections across the Amirante Passage are roughly oriented southwest to northeast, whereas those in the Mascarene Basin are oriented northwest to southeast.

izontal gradients to extrapolate into the unsampled areas, resulting in flux calculations that make consistent use of all available density information. For the mapping we assume an error-to-signal energy of 1/16 and a Gaussian covariance with 100-km lateral and 500-m vertical correlation length scales. These length scales are chosen because the shear signature of the boundary current appears to be about 100 km wide in the vicinity of the Amirante Passage and potential isopycnals fall about 500 m over that distance. Median station spacing is 33 km in the passage and the median magnitude of the bottom pressure difference between stations is 300 dbar; hence the formal errors in the bottom triangles are small because the bottom triangle regions are usually within a correlation length scale of actual station data in both the lateral and vertical directions. These small formal errors mean that data outside the bottom triangles in both directions strongly influence the mapping within them, with the ratio of their influence governed by the Gaussian covariance and their distance from the mapped region scaled by the correlation length scales.

3. Water Property Distributions

Geostrophic transport estimates often rely on water property distributions to help determine reference velocities, especially for deep currents where velocities are small. In the basins in question the bottom water, flowing from south to north, is colder, fresher, more oxygen-rich, and more silica-poor than the southward flowing deep water above it [e.g., *Wyrtki*, 1971; *Warren*, 1981; *Spencer et al.*, 1982; *Mantyla and Reid*, 1995]. The operating assumption of this interpretation of the circulation is that the water-property patterns are primarily governed by advection, so that on a given isopycnal the direction of flow tends to parallel property isopleths rather than to cross them. The reference velocities for the geostrophic velocity profiles are constrained by the velocity directions consistent with the isopycnal tracer gradients. To the extent that variable mixing along or across isopycnals influences the property distributions, the choices of reference velocities may be questionable, and, while one expects that the net flow of southern-source water should be northward, one cannot really argue that the flow everywhere should be northward. Other sources of error in inferring mean transports from synoptic surveys of the density field include time-dependent geostrophic motions such as eddies and planetary waves and ageostrophic motions such as internal waves and tides.

Isopycnal property gradients are not discernable to within measurement error and mesoscale noise below 1.6°C for the WOCE sections from within the Amirante Passage to at least 12.25°S, 55°E in the Mascarene Basin, the southeast extent of transport estimates made here. However, larger-scale distributions of water properties suggest general northward abyssal flow in this western series of basins that extends upward to depths between 3400 and 4400 m [e.g., *Wyrtki*, 1971; *Warren*, 1981; *Spencer et al.*, 1982; *Mantyla and Reid*, 1995]. Tracer data (S, O_2, and H_4SiO_4) are plotted as curves versus θ in the region of study (Figure 2) from the WOCE I7N section (Figure 3) and are also contoured in vertical sections with θ as a vertical axis over a wider latitude range (Figure 4). These data are used to support this assertion and make other inferences about deep flow directions. In addition, at least at 18°S, water characteristics of southern origin indicate northward flow as well in a thin band against Madagascar that reaches up to at least 2000 m [*Warren*, 1981].

The θ-S curves (Figure 3) for section I7N in the region of study (Figure 2) consist of a tight linear mixing line from the cold, fresh bottom end-member up to about 1.6°C. Above this mixing line is a distinct S maximum near 1.9°C. This S maximum is separated from the salty northern intermediate water above by a set of S minima that vary from 2.3° to 4.5°C. Extremely fresh minima are found between 3° and 4°C at three stations. The cold, fresh end-member near the bottom is Circumpolar Deep Water spreading northward from

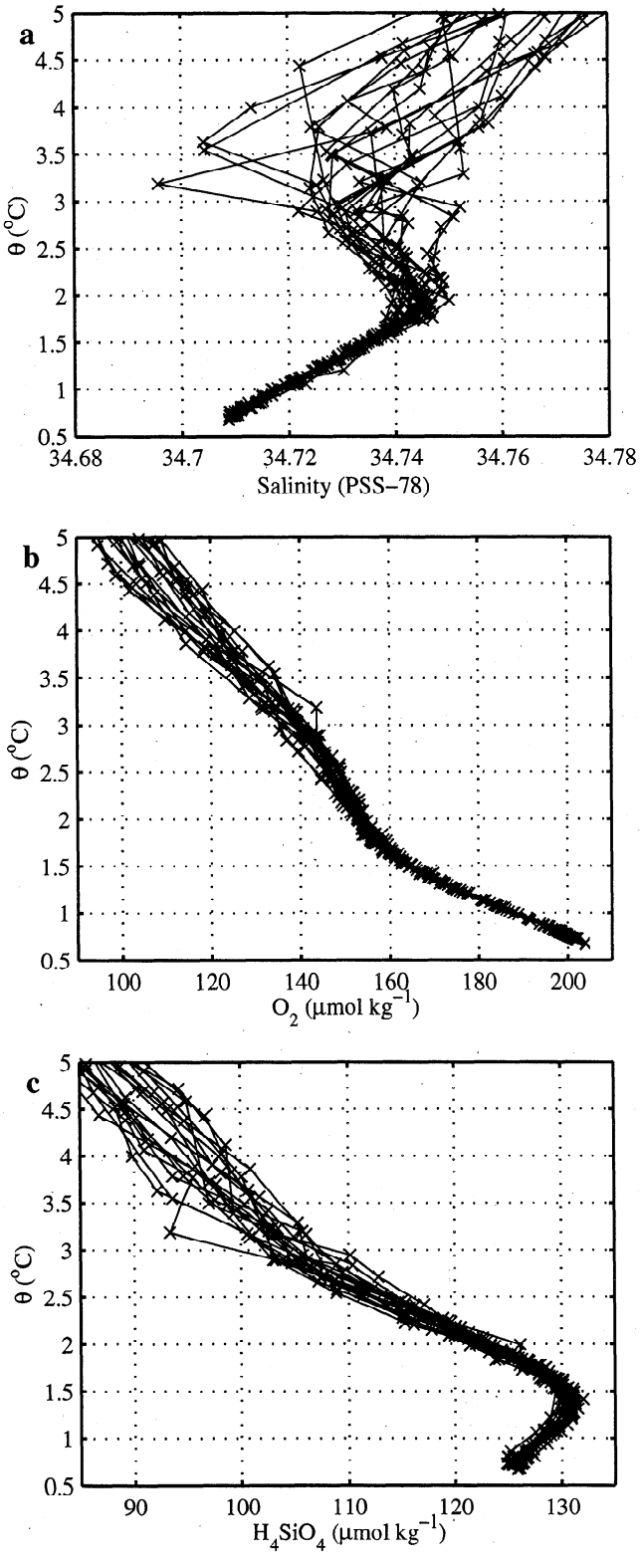

Figure 3. Property curves of (a) S, (b) O_2, and (c) H_4SiO_4 versus θ. Stations 720–738 from WOCE section I7N (open circles on Figure 2) are used. The Circumpolar Deep Water near the bottom is fresh, oxygen-rich, and relatively silica-poor compared with the Indian Deep Water with a salty, oxygen-poor, silica-rich core from 1.4°–1.9°C. A tendency toward fresh, oxygen-rich, and silica-poor values of southern origin near 3°C suggests an upper bound for the Indian Deep Water near 2.5°C.

the south (Figure 4). The S maximum near 1.9°C is a signature of the Indian Deep Water spreading southward from the north (Figure 4). The S minimum near 3°C is again suggestive of water with a southern origin located above the Indian Deep Water (Figure 4). Here the term "spreading" is used to signify the combined effects of advection and diffusion on the water property fields.

Dissolved O_2 values are highest near the bottom and, over the large scale, decrease toward the north, indicating northward spreading of oxygen-rich Circumpolar Deep Water from the south [*Toole and Warren*, 1993]. The θ-O_2 curves have a maximum curvature at about 1.6°C (Figure 3), and the low values there are suggestive of oxygen-poor Indian Deep Water spreading south from the north (Figure 4). Another curvature maximum of opposite sign near 3°C (Figure 3) again suggests either oxygen-rich water of a southern origin above the Indian Deep Water (Figure 4) or a region of little net flow. Nitrate and phosphate curves (not shown) are very strongly anticorrelated with the tendency of O_2, so they do not add much additional information.

The θ-H_4SiO_4 curves have a deep maximum near 1.4°C (Figure 3), indicating southward spreading of silica-rich Indian Deep Water of northern origin (Figure 4). Values decrease below the maximum in a relatively tight, linear fashion (Figure 3), a result of northward spreading of relatively silica-poor Circumpolar Deep Water somewhere below the H_4SiO_4 maximum (Figure 4). Again, near 3°C, there is a curve toward lower values (Figure 3), suggestive of either the influence of silica-poor waters of southern origin above the Indian Deep Water H_4SiO_4 maximum (Figure 4) or little net flow in this temperature range.

The planetary component of potential vorticity Q is another conservative tracer in the absence of mixing, friction, or significant relative vorticity [*Pedlosky*, 1987]. Here $Q = f/gN^2$, where f is the local Coriolis parameter. Overall, there is an interior minimum in the magnitude of Q between 1.4° and 1.6°C, and magnitudes are again very low near the ocean floor (Figure 5). Above 1.6°C, magnitudes increase toward the main pycnocline. There is an interior maximum near 1°C.

Maps of Q on three deep isopycnal surfaces have been published for the Indian Ocean [*O'Dwyer and Williams*, 1997, Figures 8b, 11b, and 15b]. These isopycnal surfaces are near $\theta = 1.85°$, 1.35°, and 1.15°C in the region of study. While they are not ideal for tracing the extrema described above, the lightest surface, with lowest magnitudes of Q from the equator to 30°S found in the western basin system, suggests that the interior minimum at 1.4° to 1.6°C (Figure 5) is a signature of a plume of southward flowing Indian Deep Water. Indian Deep Water originating in the north with a small positive Q and moving southward would have to modify Q to a small negative value near the equator by mixing processes, probably at the western boundary, as seen from 1.4° to 1.6°C. Near the bottom in the Circumpo-

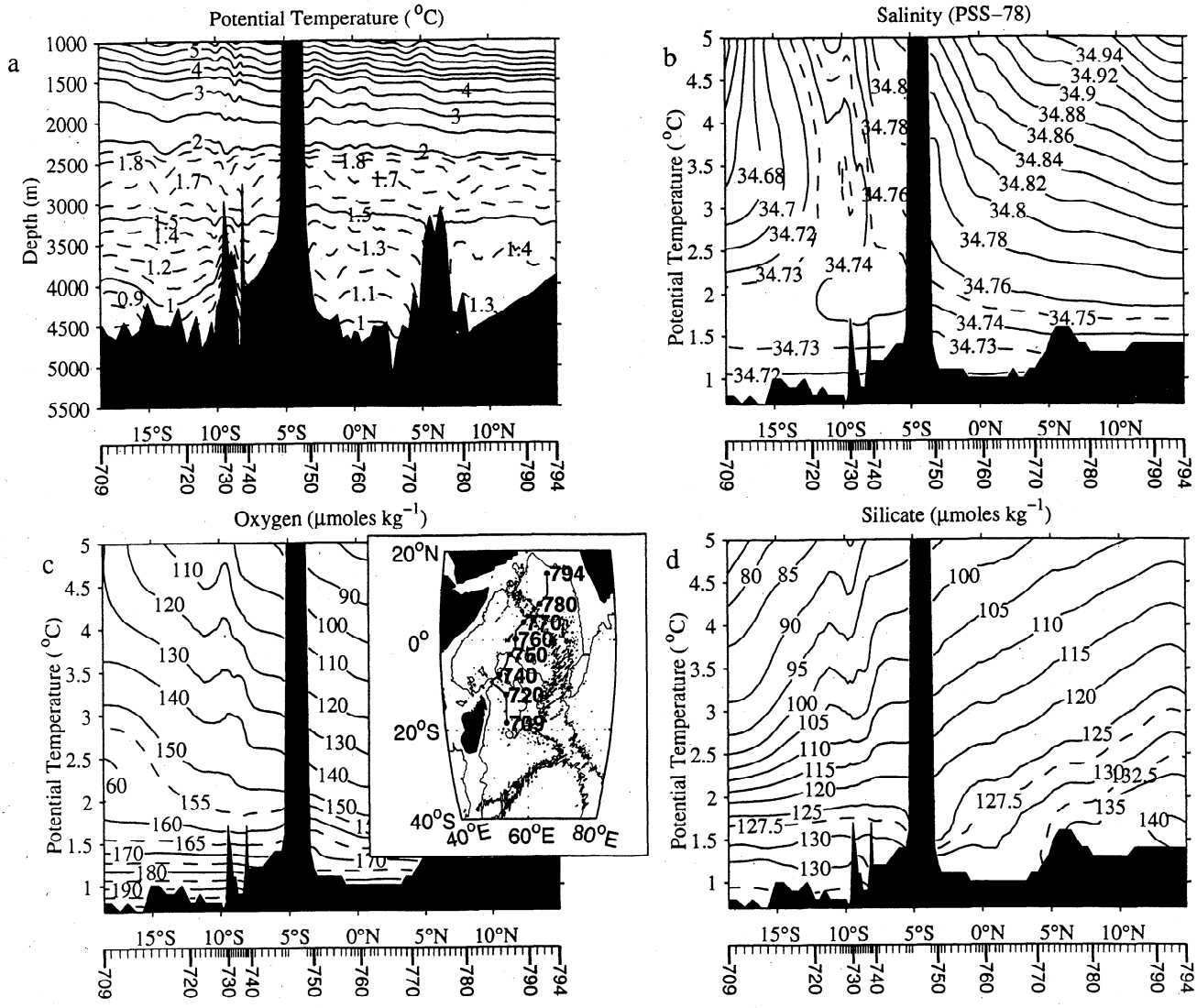

Figure 4. Distribution of deep water properties along I7N from station 709 in the Mascarene Basin to station 794 in the Arabian Sea: (a) vertical section of objectively mapped θ contoured with depth as the vertical axis, (b) vertical section of S with θ as the vertical axis, (c) vertical section of O_2 with θ as the vertical axis, and (d) vertical section of H_4SiO_4 with θ as the vertical axis. Station locations are given at the bottom of each plot. Bottle S, O_2 and H_4SiO_4 are linearly interpolated to θ at each station and then smoothed before contouring. The inset map in Figure 4c shows the station locations. The Amirante Passage is between stations 731 and 740. The topographic features near 5°S and 5°N are the Seychelles Bank and the Carlsberg Ridge, respectively.

lar Deep Water, the magnitude of Q is again reduced by vertical mixing and the no-flux bottom boundary condition, but above that a finite negative value is carried north in the Circumpolar Deep Water, corresponding to the magnitude maximum near 1.0°C. The two denser surfaces of *O'Dywer and Williams* [1997] show a similar maximum in the magnitude of Q along the western boundary, just east of Madagascar, consistent with a Circumpolar Deep Water influence spreading northward in the Western Basin.

An alternate explanation of similar maxima in the magnitude of Q in the Pacific Ocean is that they reveal boundaries between homogenous water masses of Circumpolar Deep Water flowing north and Pacific Deep Water flowing south [*Reid and Lonsdale*, 1974], rather than a core layer of high-magnitude Q water as suggested above. This hypothesis is also consistent with higher Q magnitudes near the western boundary, but the dynamical foundation for this interpretation has been called into question using models to provide counterexamples [*Warren*, 1977].

4. Volume Fluxes

Vertical sections of potential temperature (Figure 5) give a qualitative indication of where the deep geostrophic shear is located. Geostrophic shear is located where potential isotherms tilt strongly and stratifica-

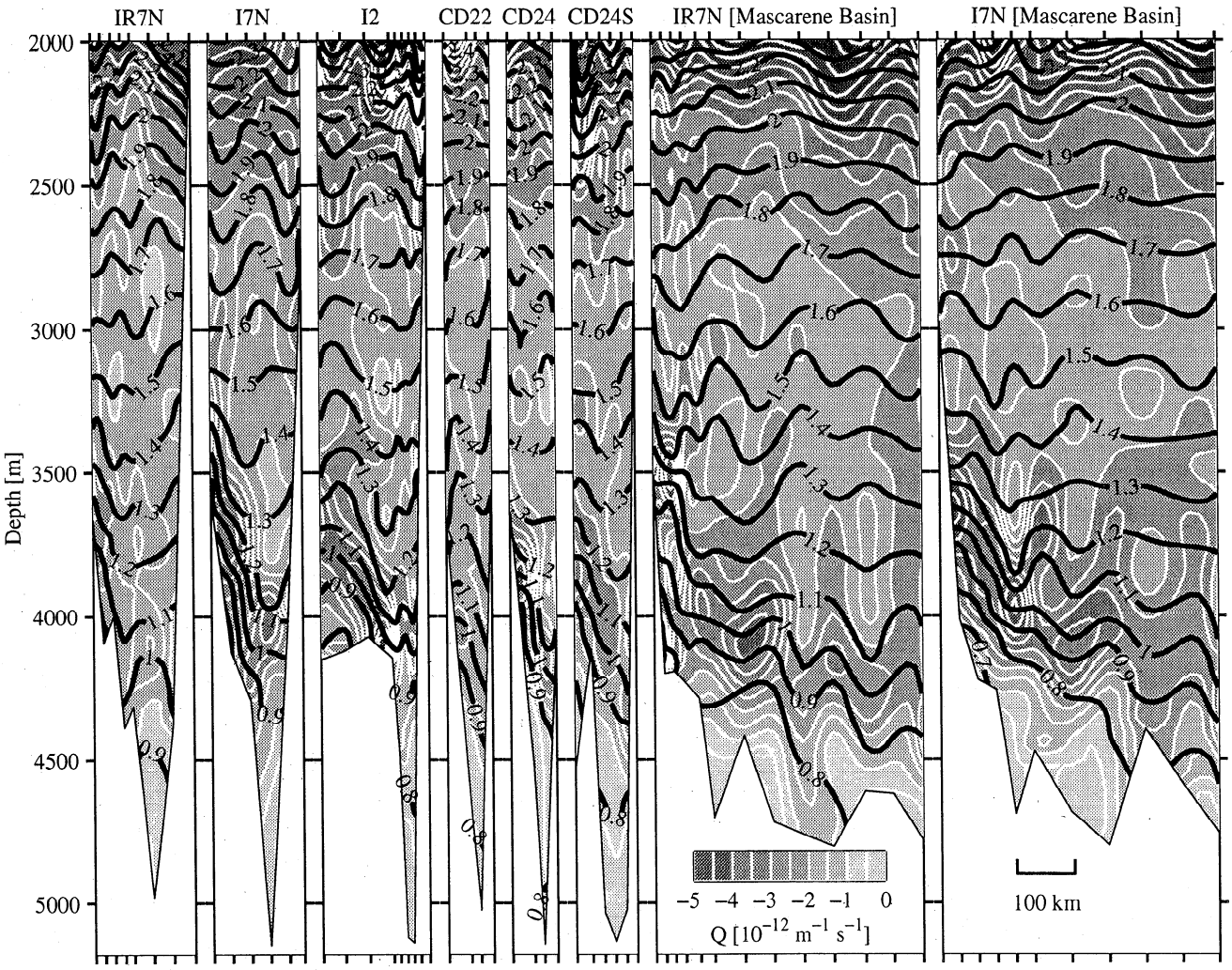

Figure 5. Deep vertical profiles of potential vorticity (Q, shaded at 1.0×10^{-12} m^{-1} s^{-1} intervals and contoured with thin white lines at 0.5×10^{-12} m^{-1} s^{-1} intervals) with potential temperature (θ, contoured with thick dark lines at 0.1°C intervals) for the hydrographic sections across the Amirante Passage (six left profiles) and Mascarene Basin (two right profiles). Station locations (see Figure 2) are shown by tick marks at the tops and bottoms of the sections. The western edge of each section is toward the left side. The vertical exaggeration is 500:1.

tion is high (hence the magnitude of Q is large), regions centered around 0.9° to 1.1°C. As detailed above, this high Q magnitude is either associated with northward flow of Circumpolar Deep Water or reveals the boundary between Circumpolar Deep Water below and Indian Deep Water above. In either case, the shear is such that overall northward velocity increases toward the bottom around these potential isotherms.

The water property distributions (Figures 3 and 4) suggest that the cold, fresh, oxygen-rich, nutrient-poor Circumpolar Deep Water should be flowing north somewhere below 1.4°C, and at the very least within the relatively homogenous bottom layer. These same distributions suggest that the warmer, saltier, oxygen-poor, nutrient-rich Indian Deep Water should be flowing south between 1.4° and 1.9°C. The property distributions, especially the salinity minimum strengthening to the south near 3°C, make an intermediate potential isotherm, 2.5°C (near 1950 m), a reasonable upper boundary for the extent of Indian Deep Water in the region.

In the absence of other information, there is no particular reason to pick a ZVS at a single P, θ, potential density, within minimum or maximum shear layers, or even assume that a ZVS exists everywhere. Here we choose to use θ surfaces for a ZVS and compute geostrophic volume transports for a set of ZVSs between 0.7° and 2.0°C at 0.1°C intervals. Where the lowest temperature is higher than the ZVS, the bottom is used as the ZVS. Use of a set of isopycnal or even level surfaces would certainly give similar results. This exercise is performed for all three WOCE sections across the Amirante Passage and the three partial historical sections there, as well as for the two WOCE sections in the Mascarene Basin. The volume transports for each section in each ZVS are summed in 0.1°C bins. The values in bins for each sec-

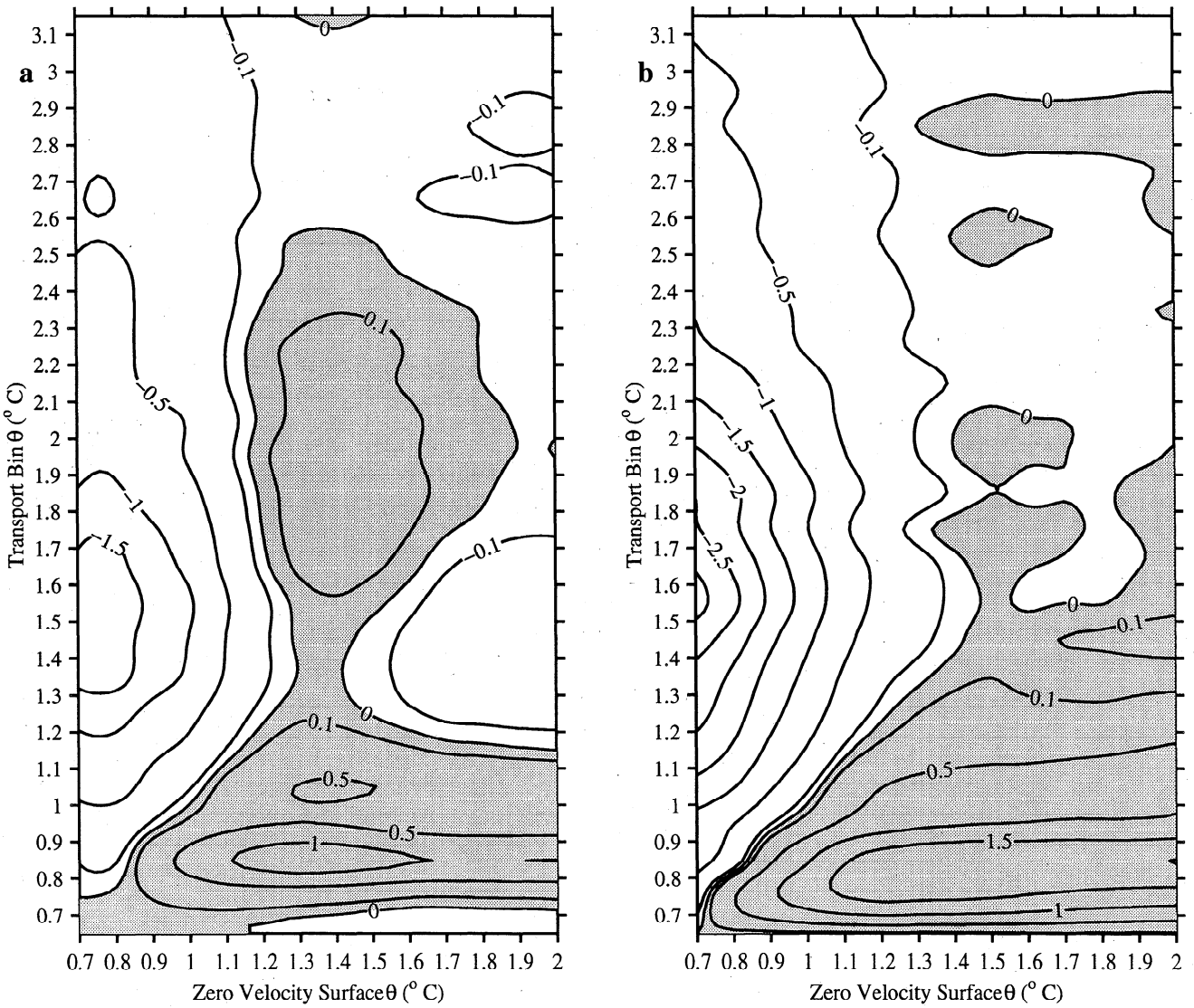

Figure 6. Contour plots of mean geostrophic volume transport (in 10^6 m^3 s^{-1}) per 0.1°C bin as a function of zero velocity surface specified by potential temperature. Regions of positive transport are shaded. The requirements that bottom water be flowing north, deep water between 1.4° and 1.9°C be flowing south, and the zero velocity surface be the same in the (a) Amirante Passage and (b) Mascarene Basin constrain the zero velocity surface to lie between 0.9° and 1.1°C.

tion are then averaged to find mean volume transports (Figure 6) and standard deviations (not shown) in the passage and the basin, with allowances made for the partial nature of the coverage of the Amirante Passage by the older sections.

An examination of the mean transports (Figure 6) suggests that to obtain flows in the Amirante Passage and the Mascarene Basin that are consistent with the water properties in an overall sense (significant northward flow at the bottom, southward flow from 1.4° to 1.9°C), the ZVS must reside between 0.9° and 1.1°C, that is, within the region of deep geostrophic shear. With a ZVS at a lower temperature there is little or no northward bottom flow of Circumpolar Deep Water in the Amirante Passage. With a ZVS at a higher temperature some portion of the flow of Indian Deep Water between 1.4° and 1.9°C is northward in one of the locations. Estimates for ZVSs from 0.7° to 1.3°C result in a range of volume transports (Table 2). A comparison of transports between the sections can be summarized by the net transport difference between sections and the root mean square of differences between individual 0.1°C transport bins (Table 2, last column). Owing to the close proximity of the western ends of the Mascarene Basin and Amirante Passage sections (Figure 2), and the extensive shallow barrier of the Mascarene Plateau to the east (Figure 1), it seems plausible to eliminate the 0.9°C ZVS by this comparison because the transport differences for it are much larger than the 1.0° and 1.1°C ZVSs both overall and in individual bins. While there is not a large depth change over the remaining ZVS range of 1.0° to 1.1°C, it is within the high-shear

Table 2. Mean and Standard Deviations for Volume Transports (in 10^6 m^3 s^{-1}) in the Mascarene Basin and the Amirante Passage From Various ZVSs to the Bottom (Bottom Water or Circumpolar Deep Water) and From These ZVSs to 2.5°C (Deep Water or Indian Deep Water)

ZVS, °C	Mascarene Basin		Amirante Passage		Difference
	ZVS to Bottom	ZVS to 2.5°C	ZVS to Bottom	ZVS to 2.5°C	Bottom to 2.5°C
1.3	5.4 ± 1.1	−1.4 ± 0.4	2.8 ± 1.4	1.1 ± 1.0	−0.1 ± 1.7
1.2	4.8 ± 1.0	−3.3 ± 0.4	2.4 ± 1.2	−0.3 ± 1.4	−0.4 ± 1.8
1.1	3.8 ± 0.8	−6.4 ± 0.6	1.7 ± 0.9	−3.8 ± 1.9	−0.6 ± 1.6
1.0	2.5 ± 0.6	−11.6 ± 0.8	1.0 ± 0.6	−8.6 ± 2.6	−1.5 ± 1.5
0.9	1.4 ± 0.5	−17.6 ± 0.8	0.4 ± 0.3	−11.8 ± 3.2	−4.8 ± 1.9
0.8	0.5 ± 0.3	−25.2 ± 0.9	0.0 ± 0.0	−16.6 ± 3.5	−8.1 ± 2.4
0.7	0.0 ± 0.0	−31.3 ± 1.8	0.0 ± 0.0	−16.1 ± 3.2	−15.2 ± 3.9

Deviations for volume transports are given in 10^6 m^3 s^{-1}. The ZVSs shown range over most of the deep geostrophic shear. The difference column shows the net imbalance of the difference between the Mascarene Basin and the Amirante Passage between the bottom and 2.5°C with the root mean square of differences for individual 0.1°C bins between the two locations.

region (Figure 5), so small changes in ZVS depth result in large changes in transport.

Within the Amirante Passage the 1.0°–1.1°C range of ZVSs results in transports (Table 2) from 1.0 to 1.7 × 10^6 m^3 s^{-1} northward for the bottom water below the ZVSs and from 8.6 to 3.8 × 10^6 m^3 s^{-1} southward for the deep water between them and 2.5°C (the upper bound chosen for the Indian Deep Water). Fluxes in 0.1°C θ bins (Figure 7) reveal that the bulk of the bottom water transport occurs around 0.85°C, and above 0.8°C the mean fluxes exceed their standard deviations within the bottom water. In the deep water, southward transport is at a maximum at 1.55°C (Figure 7), near the core of the low-magnitude Q water. This relation is consistent with the hypothesis that this low-magnitude Q is a signature of southward spreading of Indian Deep Water (Figure 5). Below 1.6°–1.4°C, mean fluxes exceed their standard deviations in the deep water.

In the Mascarene Basin the 1.0°–1.1°C range of ZVSs results in a bottom water transport (Table 2) between the ZVSs and the sea floor from 2.5 to 3.8 × 10^6 m^3 s^{-1} northward toward the passage and a deep water transport between the ZVSs and 2.5°C from 11.6 to 6.4 × 10^6 m^3 s^{-1} southward. Fluxes in 0.1°C θ bins (Figure 7) show the most transport near 0.75°C in the bottom water, consistent with warming of bottom water from between these sections and the Amirante Passage. The maximum in southward deep water transport is again at 1.55°C, consistent with the findings in the Amirante Passage. While the small standard deviations for the Mascarene Basin suggest the two sections going into the estimate have similar geostrophic shear, much less weight should be placed on their magnitude relative to the mean than the same relation in the Amirante Passage, where statistics are derived from six sections.

A final quantity of interest is the amount of transport assigned to the bottom triangles, because that shows how much of the total estimate is dependent on the practice of objective mapping for extrapolation. In the Amirante Passage, that quantity ranges from 0.6 to 1.0 × 10^6 m^3 s^{-1} northward in the bottom water and from 0.4 to 0.1 × 10^6 m^3 s^{-1} southward in the deep water for ZVSs from 1.0° to 1.1°C. In the Mascarene Basin the transport in the bottom triangles is 0.9–1.3 × 10^6 m^3 s^{-1} northward in the bottom water and 0.2–0.2 × 10^6 m^3 s^{-1} southward in the deep water. Therefore, in the Mascarene Basin and the Amirante Passage, only a few percent of the deep water transports are estimated to reside in the bottom triangles, since little of the deep water is found in the bottom triangles. However, over half of the total bottom water transport in the Amirante Passage and a third of the bottom water transport in the Mascarene Basin are estimated to reside in the bottom triangles. Extrapolation, even if by the more sophisticated procedure of objective mapping, still accounts for a large fraction of the total bottom water transport reported in all Amirante Passage studies.

5. Discussion

At higher latitudes in the Indian and Pacific Oceans, bands of southern deep water at the western boundaries appear to flow north at middepth. Our conclusions about transports depend on identifying the ZVS with an isothermal surface, an intuitively appealing assumption with no surer computational alternative, but difficult to reconcile with data at higher latitudes. As remarked previously [*Warren*, 1981], at 18°S a thick band of relatively fresh, oxygen-rich water was interposed at middepth between Madagascar and the Indian Deep Water offshore. This feature in the water properties indicated that the Circumpolar Deep Water was flowing northward not only beneath the Indian Deep Water, but also beside and to the west of it, so that the ZVS there deviated greatly from a single isotherm. No

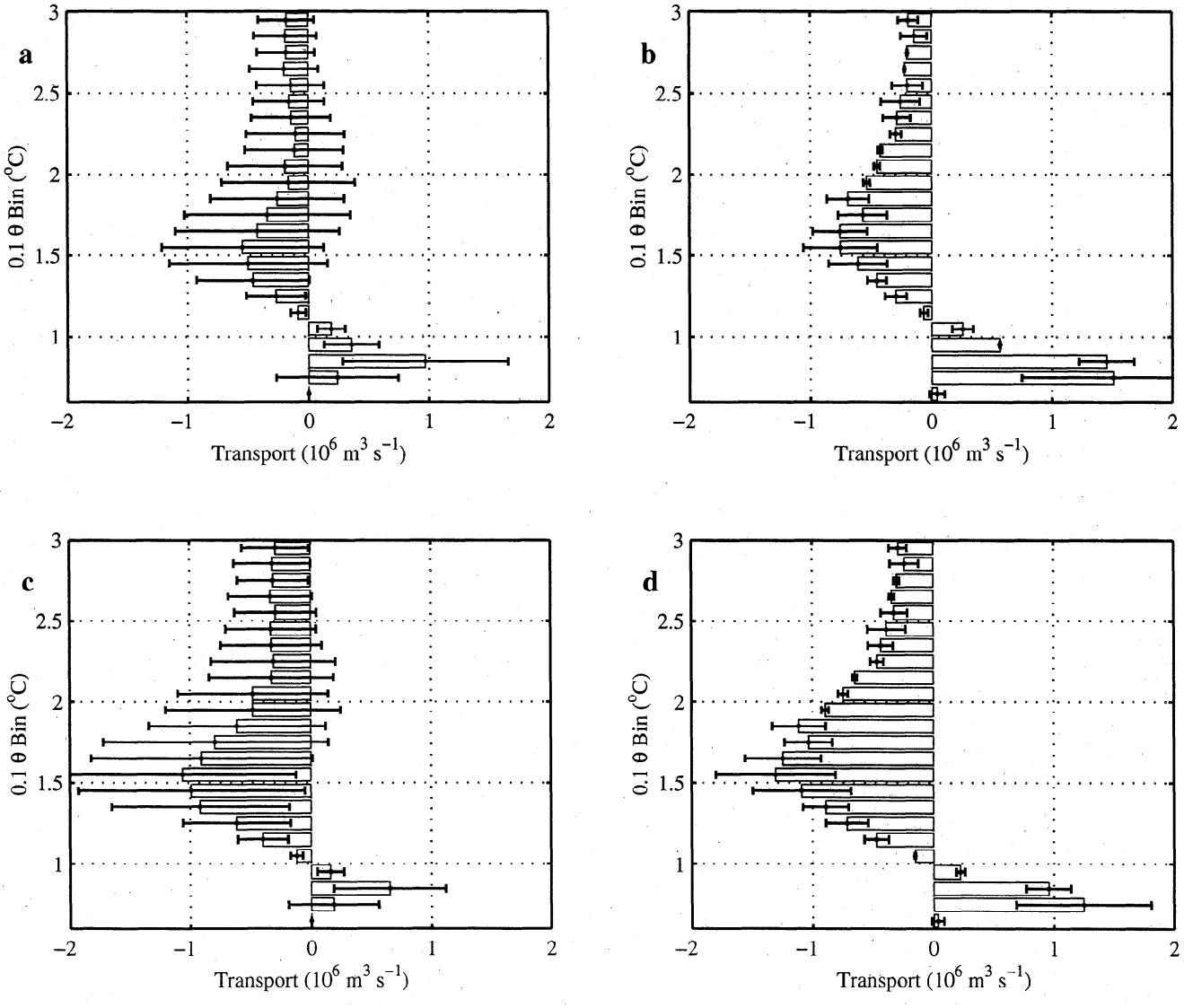

Figure 7. Plots of mean geostrophic volume transport (bars) and standard deviations (error bars) in 0.1°C bins in the Amirante Passage (Figures 7a and 7c) and Mascarene Basin (Figures 7b and 7d) for zero-velocity surfaces of 1.0°C (Figures 7c and 7d) and 1.1°C (Figures 7a and 7b). Circumpolar Deep Water flows north below the zero-velocity surfaces, and Indian Deep Water flows south above them. The net flow of Indian Deep Water southward exceeds that of the Circumpolar Deep Water northward.

such anomalous middepth feature was found near the Amirante Passage, however, so the ZVS may indeed lie close to an isothermal surface there, as assumed, but the circumstances to the south demonstrate that this need not be necessarily so. We are somewhat reassured by a potentially analogous situation in the South Pacific, where an array of deep current meters at 32.5°S reveals a narrow band of northward flowing Circumpolar Deep Water between the Kermadec Ridge and the southward flowing Pacific Deep Water offshore [*T. Whitworth III et al.*, 1998], but near 10°S in the Samoan Passage (an abyssal constriction in the South Pacific Ocean similar to the Amirante Passage in the South Indian Ocean) the ZVS appears to be well approximated by the 1.2°C potential isotherm [*Roemmich et al.*, 1996]. The fate of these narrow bands of northward flow at these low-latitude passages is uncertain. It seems possible that they may yet be found to the west of the deep passages, banked against shallower topography.

Measurements at the Samoan Passage suggest a net northward Circumpolar Deep Water transport of 7.8 $\times$ 10^6 m^3 s^{-1} [*Roemmich et al.*, 1996], several times larger than the estimate for the Amirante Passage. In addition, deep values of the chlorofluorocarbons CFC-11 and CFC-12 are undetectable in the recent WOCE surveys of the Amirante Passage. By comparison, CFC-11 has been found in the major Pacific deep western-boundary current as far north as the Samoan Passage as of March 1996 (J. Bullister, personal communication). Since the CFCs are transient tracers that are introduced

into the ocean in regions where water is exposed to the surface, this difference suggests that less Circumpolar Deep Water reaches the Amirante Passage than reaches the Samoan Passage, consistent with the transport estimates. Other possibilities for the CFC concentration contrast are that Circumpolar Deep Water reaching the Amirante Passage takes a longer path, is slower, or is diluted more with less recently ventilated waters than that reaching the Samoan Passage.

Our range of values for northward flow of Circumpolar Deep Water is at the low end of the general run of previously reported values for northward flow of abyssal water in the western basins of the Indian Ocean (Table 1). The present estimates in the Amirante Passage agree well with those of *Fieux and Swallow* [1988], but while our estimates are low because we place the ZVS within the deep shear rather than above it, theirs are likely low because the station pairs used did not completely span the passage. In contrast with our ZVS choice, the larger estimates for northward Circumpolar Deep Water flow place the ZVS mostly above the strong deep shear. Hence most previous studies implicitly underestimated the significance of southward flow of Indian Deep Water with respect to this analysis by choosing lighter ZVSs. In contrast with the historical assumption of little southward flow in the region, the estimate here is of a larger southward flow of deep water than the northward flow of bottom water beneath it (Figure 7). Given that Indian Deep Water is presumably transformed Circumpolar Deep Water returning southward, one asks how this could be. The answer may lie in the fact that the Indian Ocean has many deep basins. The aggregate of Circumpolar Deep Water upwelled in the eastern basins to a depth at which it is no longer constrained by their topography might be expected to flow westward and then return southward as Indian Deep Water in a large deep western-boundary current along Madagascar, but whether that aggregate is large enough to supply our estimated southward flow is not yet known.

The ZVS range chosen here produces noticeably smaller flows of both Circumpolar Deep Water and Indian Deep Water in the Amirante Passage than in the Mascarene Basin (Figure 7). If there is little net flow in the sides of the box defined by the sections, this result implies a significant (about 1.8×10^6 m^3 s^{-1}) conversion of Circumpolar Deep Water to Indian Deep Water in the northern Mascarene Basin, suggestive of a very vigorous meridional overturning circulation where northward flowing bottom water returns as southward flowing deep water. However, it should be noted here that a rather large gap exists between the east end of the Amirante Passage sections and the east end of the Mascarene Basin sections (Figure 2), and the difference in transports between the two sets of sections, if significant, could simply be owing to flow through this large gap.

A more complete understanding of the northward flow of bottom water and the southward flow of deep water requires a basin-wide synthesis of the WOCE Indian Ocean data. One peculiar feature in the Somali Basin that may have some bearing on the southward flow of Indian Deep Water is the strong thermostad centered near 1.5°C near 3°S off the African Coast visible in historical hydrographic sections there [*Johnson et al.*, 1991b; *Warren and Johnson*, 1992]. This bolus has not been discussed previously, but its low-magnitude Q connects it with the low-magnitude Q water traveling south through the Amirante Passage and Mascarene Basin [*O'Dwyer and Williams*, 1997]. This low-magnitude Q likely originates as a result of Indian Deep Water crossing the equator near the African Coast, or it could alternatively be supplied south of the equator by flow from the east.

As noted by previous investigators [*Fieux and Swallow*, 1988; *Barton and Hill*, 1989], flow of bottom water into the Somali Basin through the Amirante Passage has no exit save through upwelling. Using the volume of the Somali Basin below 4000 m, 1.5×10^{15} m^3, for the 1.1°C ZVS, and that below 4300 m, 0.8×10^{15} m^3, for the 1.0°C ZVS, together with the volume transports reported here for those ZVSs, gives a Circumpolar Deep Water residence time near 25 years, which could be halved or doubled by transport uncertainties. A mass budget using a basin area of 2.8 and 2.1×10^{12} m^2 for the 1.1° and 1.0°C ZVSs, respectively, requires deep upwelling velocities near 5×10^7 m s^{-1}, which again could be halved or doubled within uncertainty. Finally, applying a bottom geothermal heating of 0.05 W m^{-2} and a deep vertical temperature gradient within the basin of 4×10^{-4} °C m^{-1} [*Johnson*, 1990] to the abyssal heat budget demands heating of 0.2 and 0.6 W m^{-2} and vertical diffusivities of 1.5 and 3.5×10^{-4} m^2 s^{-1} at the 1.0° and 1.1°C ZVSs, respectively. Again, these values can be halved or doubled by the transport uncertainties. The vertical mixing estimates lie within the range of previous abyssal mixing estimates for the Somali Basin [*Fieux and Swallow*, 1988; *Barton and Hill*, 1989].

Additional evidence of significant mixing is found in the coldest water within the Amirante Trench, the isolated portion of the passage deeper than 4750 m [*Smith and Sandwell*, 1997]. This evidence is in the distribution of θ within the trench from the six sections analyzed here. In both 1987 (CD24S versus CD22 and CD24) and in 1995–1996 (I2 versus IR7N and I7N), θ within the trench increases by about 0.04°C over about 100 km from south to north with little indication of temporal variability, suggesting strong mixing near the bottom there, heating the abyssal water as it flows northward. A heat budget for the near-bottom isotherms in the vicinity of the Samoan Passage also implies significant mixing in the coldest water there [*Roemmich et al.*, 1996].

Acknowledgments. G.C.J. was funded by the National Oceanic and Atmospheric Administration Office of Global Programs through the Climate and Global Change Program. A.F. was funded through NOAA grant NA66GP0267. D.L.M., B.A.W., and D.B.O. were funded by the National Science Foundation through grants OCE-9401989, OCE-9413156, and OCE-9413165, respectively. None of this analysis would have been possible without the hard work on the part of the shipboard scientific parties, the officers and crew of the R/V *Knorr* and NOAA Ship *Malcolm Baldrige*, and those who helped to calibrate, process, and analyze the data after the completion of the cruises. PMEL contribution 1872.

References

Barton, E. D., and A. E. Hill, Abyssal flow through the Amirante Trench (western Indian Ocean), *Deep Sea Res., Part A, 36*, 1121–1126, 1989.

Fieux, M., and J. C. Swallow, Flow of deep water into the Somali Basin, *Deep Sea Res., Part A, 35*, 303–309, 1988.

Fieux, M., F. Schott, and J. C. Swallow, Deep boundary currents in the western Indian Ocean revisited, *Deep Sea Res., Part A, 33*, 415–426, 1986.

Fu, L.-L., Mass, heat and freshwater fluxes in the South Indian Ocean, *J. Phys. Oceanogr.*, *16*, 1683–1693, 1986.

Johnson, G. C., Near-Equatorial Deep Circulation in the Indian and Pacific Oceans, Ph.D. thesis, 157 pp., MIT/WHOI, Joint Program in Oceanogr., Woods Hole, Mass., 1990.

Johnson, G. C., B. A. Warren, and D. B. Olson, A deep boundary current in the Arabian Basin, *Deep Sea Res., Part A, 38*, 653–661, 1991a.

Johnson, G. C., B. A. Warren, and D. B. Olson, Flow of bottom water in the Somali Basin, *Deep Sea Res., Part A, 38*, 637–652, 1991b.

Lee, T., and J. Marotzke, Inferring meridional mass and heat transports of the Indian Ocean by fitting a general circulation model to climatological data, *J. Geophys. Res.*, *102*, 10,585–10,602, 1997.

Mantyla, A. W., and J. L. Reid, On the origins of deep and bottom waters of the Indian Ocean, *J. Geophys. Res.*, *100*, 2417–2439, 1995.

O'Dwyer, J., and R. G. Williams, The climatological distribution of potential vorticity over the abyssal ocean, *J. Phys. Oceanogr.*, *27*, 2488–2506, 1997.

Pedlosky, J., *Geophysical Fluid Dynamics*, 710 pp., Springer-Verlag, New York, 1987.

Quadfasel, D., J. Fischer, F. Schott, and L. Stramma, Deep water exchange through the Owen Fracture Zone in the Arabian Sea, *Geophys. Res. Lett.*, *24*, 2805–2808, 1997.

Reid, J. L., and P. F. Lonsdale, On the flow of water through the Samoan Passage, *J. Phys. Oceanogr.*, *4*, 58–73, 1974.

Robbins, P. E., and J. M. Toole, The dissolved silica budget as a constraint on the meridional overturning circulation of the Indian Ocean, *Deep Sea Res., Part I, 44*, 879–906, 1997.

Roemmich, D., Optimal estimation of hydrographic station data and derived fields, *J. Phys. Oceanogr.*, *13*, 1544–1549, 1983.

Roemmich, D., S. Hautala, and D. Rudnick, Northward abyssal transport through the Samoan passage and adjacent regions, *J. Geophys. Res.*, *101*, 14,039–14,055, 1996.

Smith, W. H. F., and D. T. Sandwell, Global sea floor topography from satellite altimetry and ship depth soundings, *Science*, *277*, 1956–1962, 1997.

Spencer, D., W. S. Broecker, H. Craig, and R. F. Weiss, *GEOSECS Indian Ocean Expedition*, vol. 6, *Sections and Profiles*, 140 + xiv pp., Nat. Sci. Found., Washington, D. C., 1982.

Stommel, H., and A. B. Arons, On the abyssal circulation of the world ocean, I, Stationary planetary flow patterns on a sphere, *Deep Sea Res.*, *6*, 140–154, 1960.

Swallow, J. C., and R. T. Pollard, Flow of bottom water through Madagascar Basin, *Deep Sea Res., Part A, 35*, 1437–1440, 1988.

Toole, J. M., and B. A. Warren, A hydrographic section across the subtropical South Indian Ocean, *Deep Sea Res., Part I, 40*, 1973–2019, 1993.

Warren, B. A., Deep flow in the Madagascar and Mascarene basins, *Deep Sea Res., Part A, 21*, 1–21, 1974.

Warren, B. A., Shapes of deep density-depth curves, *J. Phys. Oceanogr.*, *7*, 338–344, 1977.

Warren, B. A., Bottom water transport through the Southwest Indian Ridge, *Deep Sea Res.*, *25*, 315–321, 1978.

Warren, B. A., Transindian hydrographic properties at Lat. 18°S: Property distributions and circulation in the South Indian Ocean, *Deep Sea Res., Part A, 28*, 759–788, 1981.

Warren, B. A., and G. C. Johnson, Deep currents in the Arabian Sea in 1987, *Mar. Geol.*, 104, 279–288, 1992.

Whitworth, T., III, B. A. Warren, W. D. Nowlin, Jr., S. B. Rutz, R. D. Pillsbury, and M. L. Moore. On the deep western-boundary current in the Southwest Pacific Ocean, *Prog. Oceanogr.*, in press, 1998.

Wyrtki, K., *Oceanographic Atlas of the International Indian Ocean Expedition*, 521 + xi pp., Super. of Doc., U.S. Gov. Print. Off., Washington, D. C., 1971.

A. Ffield, Lamont-Doherty Earth Observatory, Columbia University, Palisades, NY 10964. (e-mail: affield@ldeo.columbia.edu)

G. C. Johnson, Pacific Marine Environmental Laboratory, NOAA, 7600 Sand Point Way, NE, Building 3, Seattle, WA 98115-0070. (e-mail: gjohnson@pmel.noaa.gov)

D. L. Musgrave, University of Alaska Fairbanks/SFOS, P.O. Box 757220, Fairbanks, AK 99775-7220. (e-mail: musgrave@ims.alaska.edu)

D. B. Olson, Rosenstiel School of Marine and Atmospheric Science, University of Miami, 4600 Rickenbacker Causeway, Miami, FL 33149. (e-mail: don@loquat.rsmas.miami.edu)

B. A. Warren, Department of Physical Oceanography, Woods Hole Oceanographic Institution, Woods Hole, MA 02543. (e-mail: bwarren@whoi.edu)

(Received August 19, 1997; revised August 10, 1998; accepted September 10, 1998.)